Mechanics and Mechanical Engineering
Vol. 22, No. 4 (2018) 1273–1285

https://doi.org/10.2478/mme-2018-0098

Experimental Method of Tribological Modelling of Different Coatings of Stainless Steel

Kaid-Ameur Djilali
Laboratory of Industrial engineering and sustainable development (LGIDD)-University Center of Relizane Algeria
e-mail: djilalikaidameur@yahoo.fr

Mohamed Serrier
Mechanics of Structures and Solids Laboratory. Faculty of Technology-University of Sidi-Bel-Abbes, Bp 89, cité Ben M'hidi sidi- Bel-Abbes 22000-Algeria
e-mail :Moh_serier@yahoo.fr

Received (26 May 2017)
Revised (25 May 2018)
Accepted (30 August 2018)

Fretting wear is a unique form of material degradation caused by small amplitude oscillatory relative motion of two surfaces in contact. Fretting wear is typically encountered at relative displacements of less than 300 μm and occurs in either a gross slip regime [1] (where there is slip displacement across the whole contact), or a partial slip regime (where there are parts of the contact where no slip displacement occurs). Fretting wear is experienced within a wide range of industrial sectors, [2] including aero engine couplings, locomotive axles and nuclear fuel casings [3]. Under higher loads and smaller displacement amplitudes, the contact will be within the partial slip regime, often resulting in fretting fatigue where the dominant damage mode is a reduction in fatigue life [4]. Friction is a very common phenomenon in daily life and industry, which is governed by the processes occurring in the thin surfaces layers of bodies in moving contact. The simple and fruitful idea used in studies of friction is that there are two main non-interacting components of friction, namely, adhesion and deformation [5, 6].

Keywords: coattings, stanless steel, fretting, wear, tribological behavior, design of experiments method.

1. Introduction

Wear modelling will not be possible until each step in the process of wear particle formation and elimination is clearly identified and understood. This means that the process which induces the detachment of a particle must be clearly understood, as well as the rheology of the particle in contact and the elimination process out of the contact [7]. The first step is often related to one of the well-established wear mechanisms (adhesion, abrasion, fatigue, ...) which can be described from an

accurate analysis of stresses and temperature developed within the contact. Lack of modelling is widely acknowledged in the case of fretting. In the cases of both fretting-wear and fretting-fatigue, a third-body approach is a basic need, since a particle must stay for a certain period in the interface before being ejected. Wear induced by fretting has been described in fretting maps [8].

The influence of specimen hardness steel-on-steel fretting contact was examined. In equal-hardness pairs, a variation in the wear volume of around 20% across the range of hardnesses examined was observed. However, in pairs where the two specimens in the couple had different hardnesses, a critical hardness differential threshold existed, above which the wear was predominantly associated with the harder specimen (with debris embedment on the softer specimen surface) [9].

This layer is called the tribologically transformed structure or. Understanding the mechanisms of formation of the "tribologically transformed structure or" is a key-step in the modelling of wear. Formation is considered as the first step to establish the third-body layer (powder bed) which usually separates the two contacting surfaces and in which the displacement can be accommodated Fig. 1.

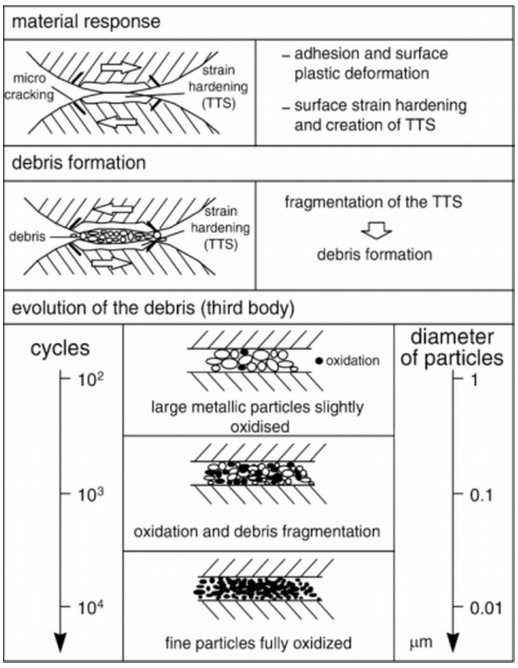

Figure 1 Creation and evolution of the third body through the contact interface

2. Experimental Investigation

The comparative study of the tribological behavior of various developed coatings on stainless steel Z30C13 fusion with laser material-supply leads to the following conclusions, knowing that their prior structural analysis indicates that it is α-Fe (Cr) Metal-borures one hand, of α-Fe composite (Cr)-h-BN on the other hand [2]:

- dry friction ruby ball (diameter 6mm, normal load $N = 1$) is reduced appreciably, the friction coefficient from 1.0 (untreated steel Z30C13) to about 0.8in the best cases;

- The wear resistance under dry friction coated steel Z30C13 strengthened considerably, since in the best cases the volumetric wear rate divided by fifty. Sliding the ruby ball on surfaces treated with laser fusion is performed under various loads to quantify wear and the energy dissipated during friction. The applied loads are 1, 2, 5 and the tests are performed on BN7 (the metal-ceramic composite), coatings and B6(the alloy boride), with the lowest wear rate under a load of 1N and stainless steel Z30C13 untreated (NF A 35573)as a control [8].

2.1. *Influence of Charge on the Tribological Behavior*

2.1.1. *Quantification of Wear*

The volumetric wear rate K_{US} in Tab. 1 are estimated as before from cross micro-profile-metrics recordings of the wear track. The changing function of the load wear rate is plotted in Fig. 1.

Table 1 Values of the volume wear rate as a function of the load of the three materials

		Z30C13 untreated	BN7	B6
	hardness H(GPa)	4.2 ± 0.1	10.0 ± 0.2	14.2 ± 0.4
	Yield Y(GPa)	1.4 ± 0.1	3.3 ± 0.1	4.7± 0.2
volumetric wear rate	1N	21.0 ± 2.2	0.6 ± 0.2	0.6 ± 0.1
	2N	37.7 ± 16.8	2.0 ± 0.9	6.3 ± 0.8
	5N	181 ± 37	11.5 ± 2.8	6.9 ± 1.7
	10N	277 ± 9	113 ± 30	92.0 ±10.3

In the case of untreated steel, the wear rate increases almost linearly with the load, to achieve $277.0 \cdot 10^{-15}$ $m^3N^{-1}m^{-1}$ under the load of 10N, while the treated samples, BN7 and B6, show a low wear rate up to 5N and do not exceed $\approx 10.0 \cdot 10^{-15}$ $m^3N^{-1}m^{-1}$. However, their rate of wear is greatly increased in 10 N and reached a value of around $100.0 \cdot 10^{-15}$ $m^3N^{-1}m^{-1}$.

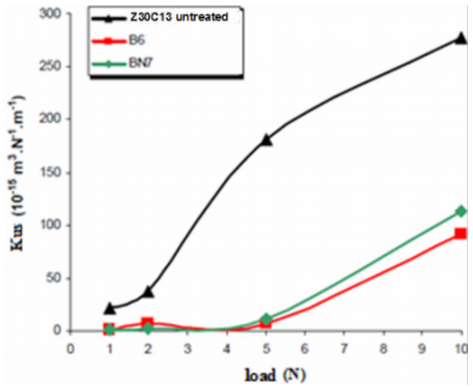

Figure 2 Evolution of the volume wear rate as a function of load

As mentioned by Blouet and Gras [3], there is a critical load beyond which the wear increases significantly in Tab. 2. In the first part of the curve, under low load, the used volume is substantially proportional to the load (up to 5N). The load increase is reflected by additional wear and possibly by increasing the number of contact points (Fig. 3) and then by increasing the density of junctions. Here, the volumetric wear rate: K_{us} (10^{-13}m^3 N^{-1} m^{-1}), contact pressure: C_P (MPa).

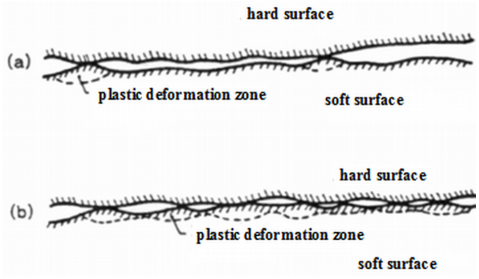

Figure 3 Body antagonists friction: (a) under low load and (b) under heavy load

Table 2 Volumetric wear rate as a function of the maximum contact pressure of three materials

Load	Sample	Yield (MPa)	C_P	K_{us}
1N	Z30C13	1400±33	498	21.0±2.2
	BN7	3333±66	514	0.6±0.2
	B6	4733±66	551	0.6±0.1
2N	Z30C13	1400±33	628	37.7±16.8
	BN7	3333±66	648	2.0±0.9
	B6	4733±66	694	6.3±0.8
3N	Z30C13	1400±33	852	181±37.0
	BN7	3333±66	879	11.5±2.8
	B6	4733±66	942	6.9±1.7
4N	Z30C13	1400±33	107	277±9.0
	BN7	3333±66	111	113±3.0
	BN6	4733±66	119	92±10.3

Fig. 4 shows that, in the contact pressure interval between 880 and 1200MPa, the wear rate of the boride coating B6 and the composite coating BN7 undergoes a drastic increase, while that of non-treated steel continues Z30C13 its almost linear growth. The maximum critical contact pressure occurs for the treated samples, as for the H13 coated steels is chromium nitride or hard chrome [8]. It is of the order of 1/11 and 1/14 of the respective hardness BN7 and B6. At these critical pressures that do not reach the limit of elasticity, plastic deformation of the sample roughness helps to increase the contact area and promotes adhesion.

Under the effect of increased stress, deterioration of sample surfaces occurs. The wear becomes more widespread, both in width and in depth (Tab. 1, Fig. 4). Except for the sample B6, 2 to 5N, the wear rate remains similar and the width and the depth of wear appear unchanged.

While the treated samples B6 and BN7 appear to have been simultaneously an adhesive and abrasive wear. This latter type of wear being suggested by the presence, on the friction surface, scratches and / or streaking caused by the hard particles of the third body [11].

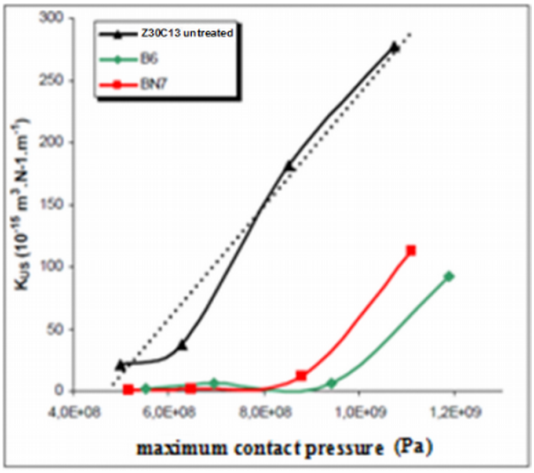

Figure 4 Evolution of the wear rate as a function of the maximum contact pressure

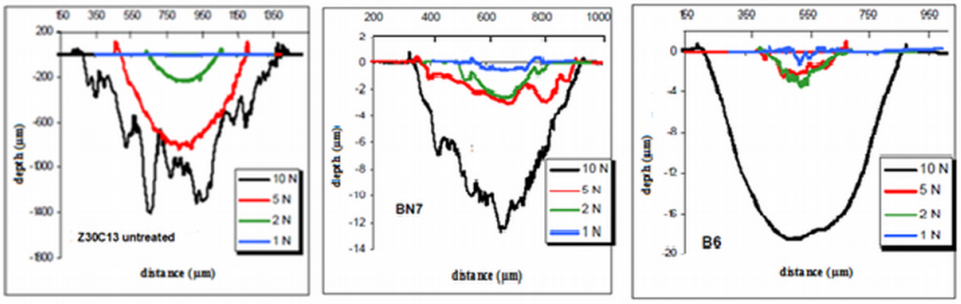

Figure 5 Wear profiles of the three materials under different loads

3. Modelling of Penetrant by the DOE Method

3.1. *Designed Experiments*

In general usage, design of experiments (DOE) or experimental design is the design of any information-gathering exercises where variation is present, whether under the full control of the experimenter or not. However, in statistics, these terms are usually used for controlled experiments. Formal planned experimentation is often used in evaluating physical objects, chemical formulations, structures, components, and materials [11].

Other types of study, and their design, are discussed in the articles on computer experiments, polls and statistical surveys(which are types of observational study),natural experiments and quasi-experiments(for example,quasi-experimental design). See Experiment for the distinction between these types of experiments or studies.

In the design of experiments, the researcher is often interested in the effect of some process or intervention (the "treatment") on some objects (the "experimental

units"), which may be people, parts of people, groups of people, plants, animals, etc. Design of experiments is thus a discipline that has very broad application across all the natural and social sciences and engineering [12].

3.2. *Principle*

There are many processes and properties that a lot is known to depend on external parameters (called factors) but we have to analytical models [13]. When it is desired to know the dependency of an output variable F of such a process or property, one is faced with several challenges:

- what are the most influential factors;
- there are interactions between factors (correlations);
- can we linearize the process (or property) depending on these factors and the resulting predictive model is it;
- how to minimize the number of measurement points of the process (or property) to obtain as much information;
- there are biases in the measurement results.

The method of experimental design addresses these issues and thus can be applied in many processes / properties that will, for example, clinical trials evaluating the quality of the most complex industrial processes [14].

3.3. *Factorial Plan (Physical Values)*

Table 3 Physical values of the parameters

Exp. No.	X_1	X_2	X_3	Y
01	4.2	1.4	1	22
02	4.2	1.4	2	37.7
03	4.2	1.4	5	181
04	10	3.3	1	0.6
05	10	3.3	2	2
06	10	3.3	5	115
07	14.2	4.7	1	0.6
08	14.2	4.7	2	6.3
09	14.2	4.7	5	69

Material: X_1, hardness: X_2, applied load: X_3, volumetric wear rate: Y. Intermediate levels:

$$X_i = \frac{u_i - \frac{1}{2}(u_{max} + u_{min})}{\frac{1}{2}(u_{max} - u_{min})} \tag{1}$$

Experience matrix (Coded Values) are shown in Tab. 4.

Table 4 Coded values of the parameter

X_1		X_2		X_3		I_{12}	I_{13}	I_{23}	Y
-1	**4.2**	-1	**1.4**	-1	**1**	1	1	1	**22**
-1	**4.2**	-1	**1.4**	-0.5	**2**	1	0.5	0.5	**37.7**
-1	**4.2**	-1	**1.4**	1	**5**	1	-1	-1	**181**
0.16	**10**	0.15	**3.3**	-1	**1**	0.024	-0.16	-0.15	**0.6**
0.16	**10**	0.15	**3.3**	-0.5	**2**	0.024	-0.08	-0.075	**2**
0.16	**10**	0.15	**3.3**	1	**5**	0.024	0.16	0.15	**115**
1	**14.2**	1	**4.7**	-1	**1**	1	-1	-1	**0.6**
1	**14.2**	1	**4.7**	-0.5	**2**	1	-0.5	-0.5	**6.3**
1	**14.2**	1	**4.7**	1	**5**	1	1	1	**69**

4. Formula Overall Mathematical Model

4.1. *Calculation Factor's Effects*

$$Y_{(n,1)} = X_{(n,p)}.a_{(p,1)} \tag{2}$$

where: $Y(n,1)$: vector responses, $X(n,p)$: matrix experience, $a(p,1)$: vector effects. Consequently

$$a = \left(X^t X\right)^{-1} X^t Y \tag{3}$$

$$(X^t X)^{-1} X^t Y =$$

$$\begin{bmatrix} 1.6962 & 1.9385 & 2.6654 & 26.9231 & 30.7692 & 42.3077 & -2.3423 & -2.6769 & -3.6808 \\ -1.8308 & -2.0923 & -2.8769 & -26.9231 & -30.7692 & -42.3077 & 2.4769 & 2.8308 & 3.8923 \\ -0.1923 & -0.0769 & 0.2692 & 0.0000 & 0.0000 & -0.0000 & -0.1923 & -0.0769 & 0.2692 \\ 0.1346 & 0.1538 & 0.2115 & 0.0000 & 0.0000 & -0.0000 & 0.1346 & 0.1538 & 0.2115 \\ 16.3462 & 6.5385 & -22.8846 & -38.4615 & -15.3846 & 53.8462 & 22.11 & 8.8462 & -30.9615 \\ -16.1538 & -6.4615 & 22.6154 & 38.4615 & 15.38 & -53.84 & -22.30 & -8.9231 & 31.2308 \end{bmatrix} \begin{bmatrix} 22 \\ 37.7 \\ 181 \\ 0.6 \\ 2 \\ 115 \\ 0.6 \\ 6.3 \\ 69 \end{bmatrix}$$

So,

Table 5 Factor's effects

Factor		Effect
The general average	a_0	42.96
Mat	a_1	-12.78
Ha	a_2	-12.77
Applied load Pa	a_3	53.20
Interaction(Mat*Ha)	I_{12}	7.44
Interaction((Mat*Pa)	I_{13}	-9.82
Interaction(Ha*Pa)	I_{23}	-9.85

4.2. *Analysis with a Single Variable Factor*

4.3. *Discussion*

The three graphs represent the evolution of the wear rate as a function of the three parameters (type of coating, surface hardness and the applied load). The first graph, we see that the wear rate decreases with the addition of steel cladding and at the same time it is much more with alloy boride (B6) then with the metal-ceramic composite (BN7). This rate is confirmed in the second graph is represented or the evolution of the wear rate according to the harshness thus showing the importance

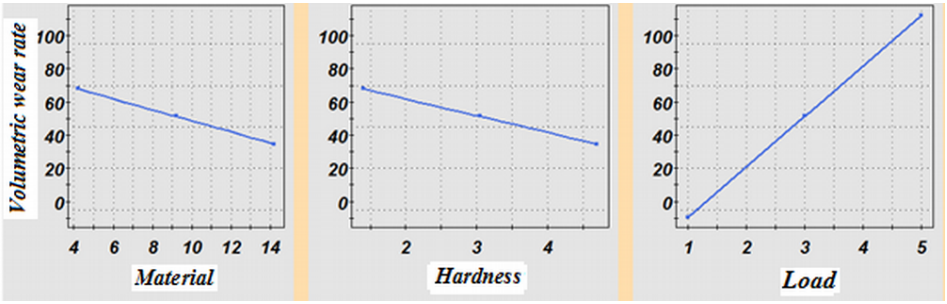

Figure 6 Evolution of the wear rate as a function of the three parameters

of anti-wear protection provided by the coating alloy boride (B6) and regresses during the coating by the metal-ceramic composite (BN7) and more uncoated.

By against the wear rate is proportional to the pressure of the load applied on the surface's steel (bare and with the two coatings) or the third graph reveals that changes in the form of a straight "linear". And by referring to the third curve whose slope is positively large compared to the other two and that are negative it is emphasized among the three parameters that affects the load applied more intensely on the wear rate.

4.4. *Analysis with Two Variable Factors*

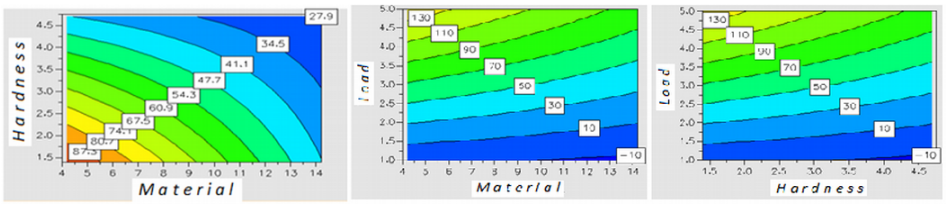

(a) (b) (c)

Figure 7 Evolution of the wear rate as a function of the two parameters [(H-M), (L-M), (H-L)]: (a) interaction (H-M); (b) interaction (L-M); (c) interaction (H-L)

Graph (a): Interaction (H-M) In this configuration, or the evolution of the wear is governed by the interaction of two of the three parameters mentioned in the previous three graphs (hardness and type of coating), or it is clear that the wear rate decreases dramatically with increasing hardness that it is related to the nature of the steel coating from the "naked" surface coating by the metal-ceramic composite (BN7) to the coating alloy boride (B6).

Graph (b): Interaction (L-M) We note that the influence of the interaction (applied load and type of material) on the wear rate is inversely; For the wear rate decreases by parabolic shape when the load falls together the merged coating the steel surface with a considerable decrease in the rate of wear which tends more

towards the melting of the alloy boride (B6) through the coating by the metal-ceramic composite (BN7).

Graph (c): Interaction (H-L) In this case, we note that the interaction (load applied and hardness) influences in the same way on the wear rate as in the previous representation or it is quite visible in the fall parabolic profile of the wear rate considerably more than the hardness is important with decreasing the applied load.

Finally, the effect of the first interaction (H-M) represented by the first graph, rapidly increase the rate of wear in parabolic profile unlike the other two interactions [(L-M), (L-H)] represented by the graphs 2 and 3, which decrease the rate of wear always parabolic profile but slowly.

5. Analysis with Three Variable Factors (Analysis of Variance)

$$Y = a_0 + a_1X_1 + a_2X_2 + a_3X_3 + I_{13}X_1X_3 + I_{23}X_2X_3 + e_i \tag{4}$$

Table 6 Variable's factors of ANOVA

Test N°	Y (observed)	Y (predicted)	$e = \lvert Y_{obs} - Y_{pre} \rvert$
01	22	8.36444444	13.6355556
02	37.7	44.7994444	7.09944444
03	181	154.104444	26.8955556
04	0.6	-5.68859556	6.28859556
05	2	19.3870544	17.3870544
06	115	94.6140044	20.3859956
07	0.6	-3.39555556	3.99555556
08	6.3	13.3694444	7.06944444
09	69	63.6644444	5.33555556

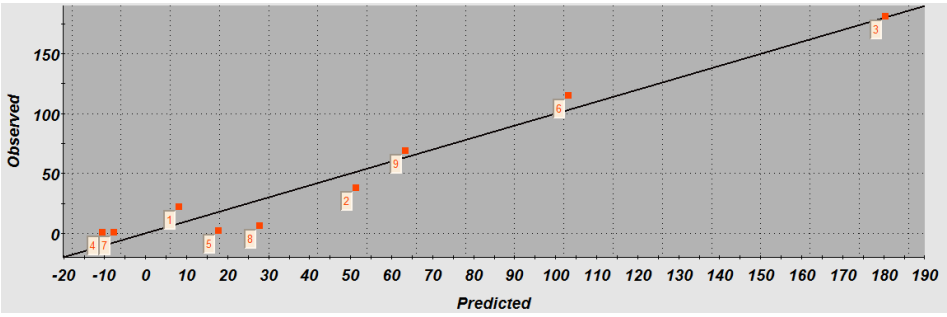

Figure 8 Distribution of the experimental points from the mathematical model; line – mathematical model, marks – experimental model

5.1. *Variation Due to the Linear Connection*

$$\text{SCEL} = \int \left(Y_i^{pred} - Y_{moy}\right)^2 \tag{5}$$

$$\begin{aligned}\text{SCEL} = \quad & (8.364 - 42.96)^2 + (44,799 - 42.96)^2 + (154.104 - 42.96)^2 \\ & +(-5.688 - 42.96)^2 + (19.38 - 42.96)^2 + (94.61 - 42.96)^2 \\ & +(-3.39 - 42.96)^2 + (13.36 - 42.96)^2 + (63.64 - 42.96)^2\end{aligned}$$

$$\text{SCEL} = 22818.81\,.$$

5.1.1. *Residual Variation*

$$\text{SCER} = \int \left(Y_i^{obs} - Y_i^{pred}\right)^2 \tag{6}$$

$$\begin{aligned}\text{SCER} = \quad & (22 - 8.36)^2 + (37.7 - 44.79)^2 \\ & +(181 - 154.10)^2 + (0.6 + 5.6)^2 + (2 - 19.38)^2 + (115 - 94.61)^2 \\ & +(0.6 + 3.39)^2 + (6.3 - 13.36)^2 + (6.3 - 13.36)^2 + (69 - 63.66)^2\end{aligned}$$

$$\text{SCER} = 1811.55\,.$$

Table 7 The commonly used analysis of variance table to gather this information

Source of variation	ddl	square sum	square means	F_{abs}
Regression model	$5(k-1)$	SCEL=22818.81	MCF=SCEL/$(k-1)$ 3803.13	MCF/MCR 6.29
Residues	2(n-k)	SCER=1811.55	MCR=SCER/(n-k) 603.85	
Total	7(n-1)			

5.2. *Output Factors (Rejection)*

The value read in the test Ficher's table of $F_{critical}$ with $(k-1)$ and $(n-k)$ degrees of freedom is equal to 5.14 and the calculated value of F_{abs} is equal to 6.29. The comparison of these two values shows that $F_{abs} > F_{crit}$ so this model is globally significant.

5.2.1. *Rejection of Factors*

This operation is important because it reduces the size of the problem by rejecting the non-significant factors by using a Student's table at $(\nu = n - p)$ degrees of freedom (n is the number of experiments carried out and the p number of effects including the constant) and a first type of risk α (usually 5 or 1%).

The test of the rule is as follows:

- If $|$ the effect of a parameter $| > t_{crit}(\alpha, \nu)$: the effect is significant.
- If $|$ the effect of a parameter $| < t_{crit}(\alpha, \nu)$: the effect is not significant.

Table 8 Results of the rule test

Factor			val. abs	test	result
The general average	a_0	42.96	42.96	42.96>18.78	significant
Mat	a_1	-12.78	12.78	12.78 < 18.78	not sign.
Ha	a_2	-12.77	12.77	12.77 < 18.78	not sign.
Applied load Pa	a_3	53.20	53.20	53.20 > 18.78	significant
Interaction Mat*Ha	I_{12}	7.44	7.44	7.44 < 18.78	not sign.
Interaction Mat*Pa	I_{13}	-9.82	9.82	9.82 < 18.78	not sign.
Interaction Ha*Pa	I_{23}	-9.85	9.85	9.85 < 18.78	not sign.

According to this test, the factors that are not relevant may be rejected that is removed from the study.

$$s_i = \frac{s}{n} \tag{7}$$

Here, s is the variance and n is the number of experiments (the test is done using so to keep the same variance throughout the model).

$$s = \frac{1}{n-p} \int e_i^2 \,. \tag{8}$$

$$S = 603.85$$

Consequently:

$$S_i = 67.09$$

And through the Student's table, the critical value is 0.28.

$$T_{crirical} * S_i = 18.78$$

The application of the rule of the test, resulting in the following:

And in this phenomena on the general average, temperature and time are significant factors that must be specified confidence interval (range where the factor is still significant) of each of the following:

$$a^{\pm Tcritical*si}$$

Then both a_0 and a_3 effects cited above are written respectively as follows:

$$45.96^{\pm 18.78},\ 53.20^{\pm 18.78}\,.$$

6. Conclusions

- Finally the experiments planning method allowed us to note that besides the direct influence of the three parameters considered on the wear rate by the graphs shown in Fig. 6 or the change rate of a linear profile descending to the first two graphs (Fig. 6) and growing at 3rd graph in the same figure, the wear rate is also governed by the influence of interactions between parameters in pairs as indicated the graphs in Fig. 7.

- This variation of the wear rate is an increasing parabolic profile in Fig. 7(a) and a descending parabolic profile in Fig. 7(b) and Fig. 7(c).

- The friction tests under different loads (1, 2, 5 and 10N) were used to characterize the wear and the dissipated energy. For coatings, the alloy boride (B6) and the metal-ceramic composite (BN7), two successive separate wear regimes appear to exist. The first is characterized by a low increase in wear when the dissipated energy increases to a value corresponding to a much greater intensification of wear, when increasing the dissipated energy is sued over this critical value.

- Under a load 1N, the friction coefficient (for dry sliding) on the ceramic coatings (ruby) is reduced, 0.8 in the best of cases, compared to 1.0 coefficient obtained with the untreated steel Z30C13. Under different loads from 1 to 10N, the tribological behavior of the coatings having the highest wears resistance.

References

[1] **Budinski, K.G.**: Guide to Friction, Wear and Erosion Testing: (MNL56), *ASTM International*, **2007**.

[2] **Leen, S., Hyde, T., Ratsimba, C., Williams, E., McColl, I.**: An investigation of the fatigue and fretting performance of a representative aero-engine spline coupling, *J. Strain and Eng. Des.*, **37**, 565–583, **2002**.

[3] **Zheng, J.F., Luo, J., Mo, J.L., Peng,J.F., Jin, X.S., Zhu, M.H.**: Fretting wear behaviors of a railway axle steel, *Tribol. Int.*, **43**, 906–911, **2010**.

[4] **Lee, Y.H., Kim, H.K.**: Fretting wear behavior of anuclear fuel rod under a simulated primary coolant condition, *Wear*, **301**, 569–574, **2013**.

[5] **Vingsbo, O., Söderberg, S.**: On fretting maps, *Wear*, **126**, 131–147, **1988**.

[6] **Ashby, M.F. and Jones, D.R.**: Matériaux, Propriétés et Applications, *éd. Dunod*, Chap. 25, **1991**.

[7] **Descartes, S. and Berthier, Y.**: *Mat & Tech.,* 1-2 , p. 3-14, **2001**.

[8] **Avril, L.**: THÈSE Elaboration de revêtements sur acier inoxydable, simulation de la fusion par irradiation laser, caractérisation structurale, *Mécanique et Tribologique,* **2003**.

[9] **Blouet, J. and Gras, R.**: Revue Mécanique-Electricité, **29**, 9–28, **1969**.

[10] **Chiu, L.H., Yang, C.F., Yang, W.C.**: *Surf. Coat. Techn.*, **154**, 282–288, **2002**.

[11] **Murphy, J. et al.**: Quantification of modelling uncertainties in a large ensemble of climate change simulations, *Nature*, **430**, 768–772, **2004**.

[12] **Sobol, I.**: Sensitivity estimates for nonlinear mathematical models, *Matematicheskoe Modelirovanie*, **2**, 112–118 (in Russian); translated in English in: **Sobol, I.**: Sensitivity analysis for non-linear mathematical models, *Mathematical Modeling & Computational Experiment (Engl. Transl.),*, **1**, 407–414, **1993**.

[13] **Saltelli, A., Chan, K. and Scott, M.**: (Eds.) *Sensitivity Analysis*, Wiley Series in Probability and Statistics, New York: John Wiley and Sons, **2000**.

[14] **Saltelli, A. and Tarantola, S.**: On the relative importance of input factors in mathematical models: safety assessment for nuclear waste disposal, *Journal of American Statistical Association*, **97**, 702–709, **2000**.

[15] **Lundstedt, T.**: Experimental design and optimization, *Chemometrics and Intelligent Laboratory Systems*, **42**(1-2), 3–40, **1998**.

[16] **Kleijnen, J.P.C.**: *Handbook of Simulation: Principles, Methodology, Advances, Applications, and Practice, Experimental Design for Sensitivity Analysis, Optimization, and Validation of Simulation Models*, 173–223, **2007**.